Telomere tethering at the nuclear periphery is essential for efficient DNA double strand break repair in subtelomeric region

Pierre Therizols,[1] Cécile Fairhead,[1] Ghislain G. Cabal,[2] Auguste Genovesio,[3] Jean-Christophe Olivo-Marin,[3] Bernard Dujon,[1] and Emmanuelle Fabre[1]

[1]Unité de Génétique Moléculaire des Levures (URA 2171 Centre National de la Recherche Scientifique, UFR 927 Université Pierre et Marie Curie), Département Structure et Dynamique des Génomes, Institut Pasteur, 75724 Paris Cedex, France
[2]Unité de Biologie Cellulaire du Noyau, Département Biologie Cellulaire et Infection, Institut Pasteur, 75724 Paris Cedex, France
[3]Unité d'Analyse d'Images Quantitative, Département Biologie Cellulaire et Infection, Institut Pasteur, 75724 Paris Cedex, France

In the yeast *Saccharomyces cerevisiae* that lacks lamins, the nuclear pore complex (NPC) has been proposed to serve a role in chromatin organization. Here, using fluorescence microscopy in living cells, we show that nuclear pore proteins of the Nup84 core complex, Nup84p, Nup145Cp, Nup120p, and Nup133p, serve to anchor telomere XI-L at the nuclear periphery. The integrity of this complex is shown to be required for repression of a *URA3* gene inserted in the subtelomeric region of this chromosome end. Furthermore, altering the integrity of this complex decreases the efficiency of repair of a DNA double-strand break (DSB) only when it is generated in the subtelomeric region, even though the repair machinery is functional. These effects are specific to the Nup84 complex. Our observations thus confirm and extend the role played by the NPC, through the Nup84 complex, in the functional organization of chromatin. They also indicate that anchoring of telomeres is essential for efficient repair of DSBs occurring therein and is important for preserving genome integrity.

Introduction

Elucidation of spatial organization of chromosomes in the cell nucleus and the consequences on chromosome metabolism is an area of intense research. In many organisms, chromosomes adopt a preferential spatial arrangement (Cremer and Cremer, 2001; Marshall, 2002). This is also observed to a certain extent in the nuclei of the yeast *Saccharomyces cerevisiae*, with centromeres found at one pole of the cell, the nucleolus—and therefore rDNA—at the opposite pole, while the 32 telomeres cluster in 4–8 foci close to the nuclear periphery (Gotta et al., 1996; Jin et al., 2000).

Two out of these three chromosomal regions, namely telomeres and the rDNA locus, are characterized by their ability to epigenetically silence PolII-driven markers inserted therein (Gottschling et al., 1990; Smith and Boeke, 1997). This is also true in the silent mating cassettes *HML* and *HMR* (Rine and

Herskowitz, 1987). Apart from the rDNA, which follows specific silencing rules (Smith and Boeke, 1997), these domains are found at the nuclear periphery where pools of silent information regulator (Sir1-4) proteins, essential for establishment and maintenance of telomeric and *HM* silencing, are concentrated (Gotta et al., 1996). In certain experimental systems, delocalization of silencing factors can repress nontelomeric or silencer-deficient loci (Maillet et al., 1996, 2001; Marcand et al., 1996; Feuerbach et al., 2002), and Sir-mediated repression of an *HMR* locus with a defective silencer is improved if the locus is brought to the nuclear periphery (Andrulis et al., 1998). However, anchoring to the nuclear envelope and silencing can be separated (Tham et al., 2001; Hediger et al., 2002b; Taddei et al., 2004). Anchoring of telomeres is mediated by at least two partially redundant pathways requiring either yKu or Sir4p and their interacting partner Esc1p (Andrulis et al., 2002; Hediger et al., 2002b; Taddei et al., 2004). Surprisingly, neither of these proteins is an integral membrane protein, although indications exist that Esc1p might behave as a membrane protein (Andrulis et al., 2002; Taddei et al., 2004). In *S. cerevisiae*, the nuclear pore complex (NPC) has been recently shown to be involved in chromatin anchoring through establishment of a nonsilenced
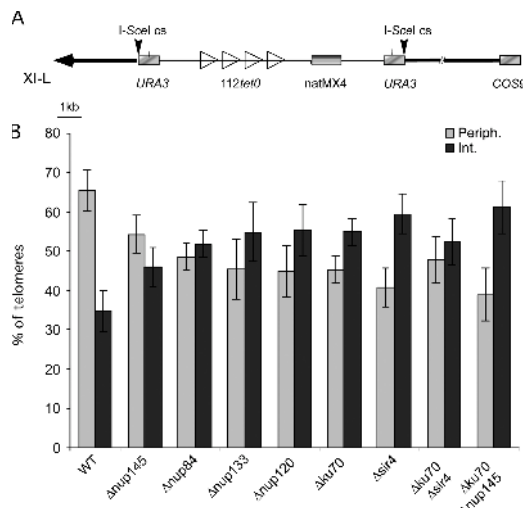
Figure 1. **Nup84 complex is required for tethering of tel-XIL at the periphery.** (A) Map of *tetO* integration site on chromosome *XI-L*. One *tetO* tract of 112 repeats is integrated 3.5 kb from the telomere of left arm of chromosome XI (XI-L). Gray rectangles, genes; open triangles, integrated *tetO* sequences; heavy black line, chromosome; thin black line, plasmid sequence; horizontal black arrow, telomere; vertical black arrows, I-SceI cutting sites. Scale in kilobases (kb) is indicated. *COS9* (*YKL219w*) is located 14.5 kb from the telomere; double slash indicates an interruption in the chromosome representation. (B) Proportion of telomeres found in each volume of the nucleus in the different genetic backgrounds. Standard errors with a P value of 0.05 are shown. Light gray columns represent values observed in peripheral volume, dark gray columns in the internal one.

domain within the silent mating-type locus *HML*, association with highly transcribed genes, and repression of telomeric domains (Galy et al., 2000; Ishii et al., 2002; Casolari et al., 2004).

In addition to its role in telomere anchoring, yKu plays a major role in double-strand break (DSB) repair. In eukaryotes, DSBs are repaired by two pathways: homologous recombination (HR) and nonhomologous end joining (NHEJ). NHEJ involves a Ku heterodimer-dependent rejoining of the two chromosome ends; HR requires a homologous region and the concerted action of proteins of the Rad52p epistasis group. HR can occur as a gene conversion (GC) event or as break-induced replication in which one portion of the chromosome arm is entirely replicated from a homologue (Sandell and Zakian, 1993; Bosco and Haber, 1998; Ricchetti et al., 1999, 2003). In the nucleus, the sites of DSB repair are characterized by the aggregation of repair proteins into foci that can recruit multiple DSBs simultaneously as evidenced both in yeast and mammals (Aten et al., 2004; Lisby et al., 2004). It is, however, not known what defines the nuclear position of the DSB foci, beside the DSB itself (Lisby and Rothstein, 2004).

The dual involvement of yKu in telomere positioning and DSB repair, together with the recruitment of repair proteins in determined foci, suggest that links, investigated here, might exist between DNA repair and spatial positioning. To affect spatial positioning, we mutated the Nup84 complex of nuclear pore proteins, a conserved core complex formed by seven distinct entities, including Nup84p, Nup120p, Nup133p, and the carboxy-terminal part of Nup145p, Nup145Cp, this having been previously shown to be involved in telomere clustering (Siniossoglou et al., 1996; Teixeira et al., 1997; Galy et al., 2000).

DSBs were generated by in vivo expression of the I-SceI endonuclease in yeast strains containing the recognition site at defined positions. Repair mechanisms have been shown previously to differ according to the position of the DSB on a chromosome (Ricchetti et al., 2003). In haploid yeast, surviving colonies are rare and cells have exclusively repaired DSB by NHEJ, unless the DSB occurred in subtelomeres (Ricchetti et al., 2003). In these domains, in addition to NHEJ, other repair events are observed, such as break-induced replication, telomere addition, and addition of exogenous sequences. These account for a three- to fourfold higher frequency of colony formation (Ricchetti et al., 1999, 2003).

In this work we show that deletion of several components of the Nup84 complex affect telomere positioning, and that this is correlated with a defect in telomeric silencing. We also show that mutants of this complex, but not nucleoporin mutants peripheral to this complex, like Δ*nup170*, affect repair of a DSB when it is subtelomeric but not when it occurs in non-subtelomeric domains. Furthermore, we confirm that telomere tethering and subtelomeric DSB repair were linked by analyzing another mutation, Δ*esc1*. Altogether our results suggest that the NPC, through the Nup84 complex, plays an essential role in chromosome positioning, and this defines a perinuclear space required for efficient subtelomeric repair.

Results

The end of chromosome XI-L is delocalized in Nup84 complex mutants

We have chosen to tag the native left end of chromosome XI-L with *tetO* binding sites for TetR-GFP fusion (Fig. 1 A; Fig. S1, available at http://www.jcb.org/cgi/content/full/jcb.200505159/DC1). The method is based on fluorescence imaging of labeled telomere in living cells through three-dimensional (3D) focus stacks and subsequent image analysis, correcting both image and nuclei distortions (see Materials and methods). We have analyzed the 3D position of the labeled telomere in the nuclear space in a wild-type strain, in mutants of the Nup84 complex, Δ*nup145C*, Δ*nup84*, Δ*nup133*, and Δ*nup120*, as well as in Δ*yku70* and Δ*sir4*, the mutants previously shown to define two redundant pathways for anchoring of telomere VI-R and XIV-L at the periphery (Hediger et al., 2002b). The quantification of the effect on telomere localization is shown in Fig. 1 B and corresponding cumulative distribution function (CDF) of radial distances in Fig. S1. For quantification, position of the *tetO* locus was mapped into two concentric spheres of equal volume, the periphery being determined by the mean position of Spc29-GFP fusion protein (see Materials and methods). As expected, in the wild-type strain, telomere XI-L is located close to the periphery in 65.3% (±5.16; $n = 427$) of cells (values for a 95% confidence interval and the number n of analyzed nuclei are given). Strikingly, the deletion of the carboxy-terminal encoding part of *NUP145*, or deletion of *NUP84*, *NUP133*, or *NUP120* leads to the relocation of telomere XI-L in the nuclear interior with only 54.12% (±4.8; $n = 312$), 48.37% (±3.44; $n = 283$), 45.27% (±7.6; $n = 323$), and 44.83% (±6,61; $n = 313$) of tagged telomere
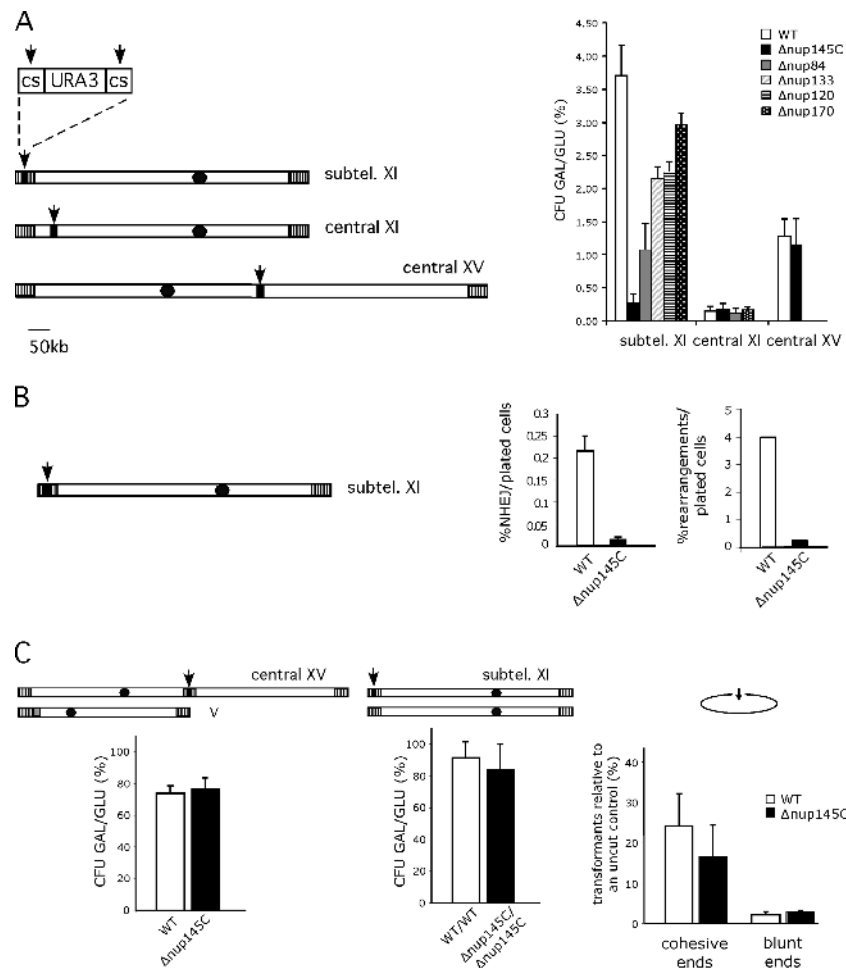
Figure 2. **Nup84 complex is required for subtelomeric DSB repair efficiencies.** (A) Survival to DSBs according to their position in wild-type and different nucleoporin mutant backgrounds. Chromosomes XI and XV are schematized. Black dots and vertical hatched boxes represent centromere and subtelomeres, respectively. Arrows indicate the positions of induced DSBs generated by cleavage of two inverted I-SceI cutting sites (cs) surrounding the *URA3* marker (black box). Size in kb is indicated. Colony forming units (CFU) are calculated as the ratio of galactose growing colonies (GAL) versus glucose growing colonies (GLU) expressed in percentages (%). Values obtained for wild-type (WT, white), Δnup145C (black), Δnup84 (gray), Δnup133 (diagonals), Δnup120 (horizontal lines), and Δnup170 (white dots) are shown according to DSB's position. Subtel. XI stands for subtelomeric XI-L. Standard errors with a P value of 0.1 are shown. (B) Proportion of repair by NHEJ and rearrangements in subtelomere XI-L. Subtelomeric DSB is schematized as in A. Percentages of repair either by NHEJ or by gross chromosomal rearrangements per plated cells are shown for wild-type (WT, white) and Δnup145C (black) (C). Repair machinery is functional in Δnup145C. Left; DSB is generated in a central part of chromosome XV and gene conversion is made possible because of homologous sequences present on chromosome V (gray box, see text and Karathanasis and Wilson, 2002). Colony forming units are calculated as in A. Middle; DSB is generated in the subtelomeric position in diploid wild-type cells or diploid cells homozygous for Δnup145C. Colony forming units are calculated as in A. Right; DSB is created on a replicative plasmid by restriction enzymes generating cohesive or blunt ended ends. Wild-type (WT) and Δnup145C strains were transformed with equivalent amounts of supercoiled or linearized pRS316 (ARS-CEN-URA3) plasmid. The number of transformants obtained with the linearized plasmid expressed as a percentage of the number of transformants obtained with the supercoil DNA are plotted. Experiments were repeated three times and error bars represent the 95% confidence intervals.

XI-L remaining in the peripheral volume, respectively. These values are close to the ones observed in cells were the telomere anchoring pathway has been inactivated by deletion of either *YKU70* (45.11% ± 3.47; *n* = 596) or *SIR4* (40.70% ± 5.04; *n* = 322). Position of telomere XI-L was also analyzed in the Δ*yku70*Δ*nup145C* double mutant (Fig. 1 B) and found to be in the peripheral volume of 38.86% (±6.7; *n* = 261) of the mutant cells. All together, our results show that telomere XI-L is preferentially found in the outmost external volume of the nucleus and that its localization at the nuclear periphery requires both yKu70p and Sir4p, a situation reminiscent to the one observed for chromosome VI-R and XIV-L (Hediger et al., 2002b; Bystricky et al., 2005). Furthermore, our results show

that a functional Nup84 complex is required for the peripheral localization of this particular chromosome end and suggest that the NPC might be involved in telomere anchoring.

The Nup84 complex affects survival to DSBs in subtelomeres

Having shown that telomere XI-L was delocalized in Nup84 complex mutants, we investigated the efficiency of survival and repair to DSBs in these mutant backgrounds. To generate DSBs, we expressed the I-SceI endonuclease in vivo in haploid strains carrying a *URA3* marker flanked by two inverted I-SceI cutting sites at defined positions (Fig. 2 A and Ricchetti et al., 2003). Cell survival is monitored by comparing the number of colonies

Table I. **Rates of cell survival as a function of DSB localization in nup mutants**

	WT	Δnup145C	Δnup84	Δnup120	ΔDnup133	ΔDnup170
Subtelomere XI-L	3.7 ± 0.4	0.3 ± 0.1	1.1 ± 0.4	2.2 ± 0.3	2.2 ± 0.1	2.9 ± 0.2
Central XI	0.16 ± 0.06	0.19 ± 0.09	0.12 ± 0.06	nd	nd	0.17 ± 0.03
Central XV	1.3 ± 0.09	1.15 ± 0.06	nd	nd	nd	nd
Central XV (GC)	73.6 ± 4.2	77 ± 5.2	nd	nd	nd	nd

Cell survival is expressed as the ratio between the number of colonies formed after induction of I-SceI in galactose versus the number of colonies present on glucose. Standard errors with a P value of 0.1 are shown. Position of the DSB along a chromosome and number of the chromosome are indicated in the first column, GC stands for gene conversion; strain genetic backgrounds are given on the top; nd, not determined.

formed after plating on inducing (galactose) versus noninducing (glucose) conditions, whereas efficiency of DSB formation is followed by measuring the percentage of [URA⁻] colonies after replica plating (see Materials and methods). In a wild-type haploid strain, most of the cells are unable to form colonies after induction of DSBs on galactose, but survival increases by a factor of 20 when the DSB is in subtelomeres (Ricchetti et al., 2003). We analyzed survival to both a cut 3.5 kb from the left telomere (L1 in Ricchetti et al., 2003) and a cut in a central region, 64 kb from the left telomere (C5) of chromosome XI in cells mutated in the Nup84 complex and in *NUP170*, a nucleoporin peripheral to this complex. As previously shown, when the DSB happens in a central region, cell survival is very low (Fig. 2 A and Table I; Ricchetti et al., 2003). We found that cell survival is comparable between wild type, Δ*nup145C*, Δ*nup84*, and Δ*nup170* strains (Fig. 2 A and Table I). On the contrary, in the case of a subtelomeric DSB, whereas in a wild-type strain cell survival reaches ∼4% (Fig. 2 A and Table I; Ricchetti et al., 2003), it decreases by 93% and 71% in Δnup145C and Δnup84 strains, respectively, and by 42% and 41% in Δnup120 and Δnup133, while it is only partially diminished in the Δnup170 strain (20%; Table I). Therefore, in all Nup84 complex mutants tested here a defect in cell survival after generation of a DSB was observed, with survival rates of cells bearing a DSB in a central and in subtelomeric region of the same chromosome

becoming similar in Δ*nup145C* and to a lesser extent in Δ*nup84* mutants, indicating that in these mutants the dependency of the survival rate on the location of the DSB along the chromosome is abolished.

Ratios of different types of repair are unaffected in Nup84 complex mutants

The decrease in cell survival could reflect either a problem in repair efficiency or some checkpoint-related problem in response to DNA damage. The latter was excluded because the Δ*nup145C* mutant adapts and recovers subtelomeric DSB like a wild-type strain, whereas the checkpoint Δ*rad17* mutant does not (see Fig. S2, available at http://www.jcb.org/cgi/content/full/jcb.200505159/DC1; and Lee et al., 1998). We therefore analyzed the mechanisms by which the DSBs were repaired. 200 colonies that formed on galactose-containing medium were screened by PCR for possible repair by NHEJ. The absolute frequency of repair was calculated by scoring the number of positive PCRs relative to the number of plated cells (in noninducing conditions). In a wild-type strain, 0.21% (±0.039) of plated cells were repaired by NHEJ; this value remaining constant along the chromosome (Ricchetti et al., 2003; and our unpublished data). The absolute frequency of NHEJ drops to 0.014% (±0.002) in Δnup145C mutant cells when DSBs are generated close to the telomere, but not when the cut is central

Figure 3. **Sequences of the junction of NHEJ events at locus L1 in Δnup145C and proposed mechanisms of NHEJ.** Coordinates of the L1 locus on chromosome XI-L are shown. I-SceI restriction sites (in opposite orientations) are in bold, cleavage position generating 4-bp 3′ overhangs is indicated by a staggered line, BamHI and KpnI restriction sites are boxed and plasmid sequences are in lower case letters (see Fairhead et al., 1996 for construction details). Possible end processing and subsequent alignment of complementary base pairs are shown. See text for details.
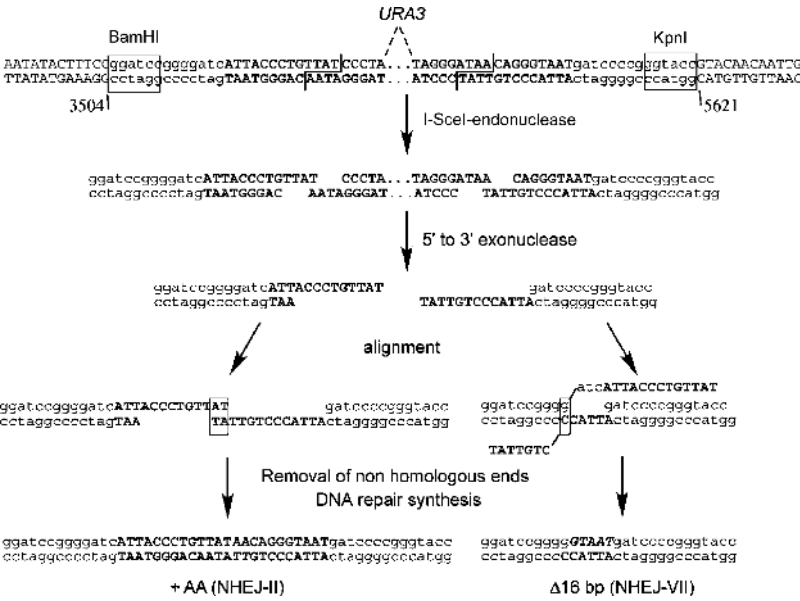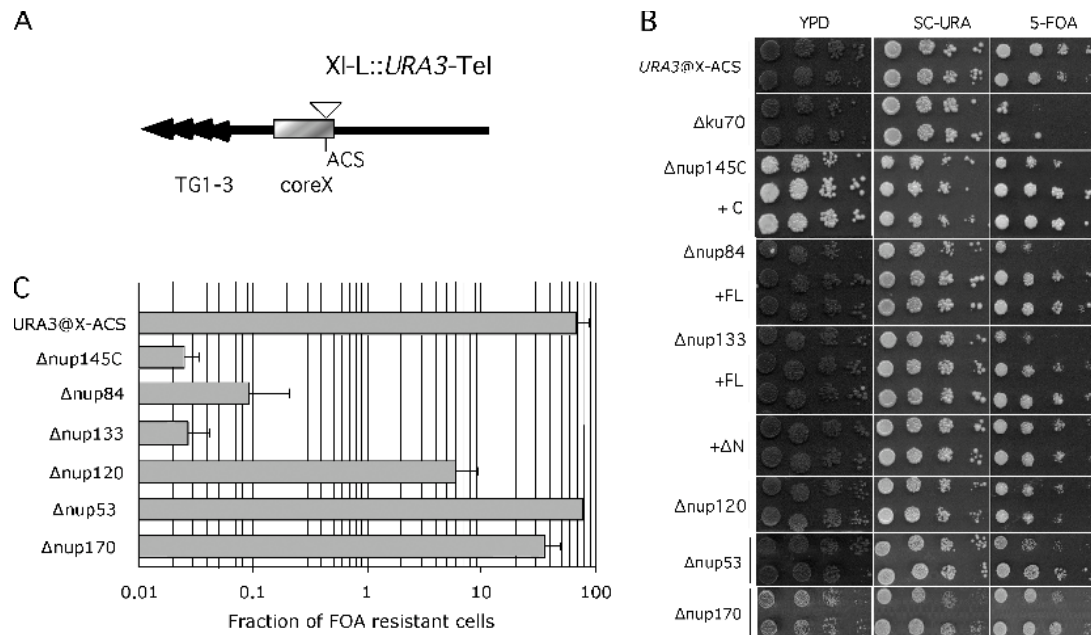
Figure 4. **Mutants of the Nup84 complex are defective for subtelomeric silencing.** (A) The native configuration of chromosome XI-L subtelomere is schematized. Black arrows represent TG1-3 repeats; gray box, the coreX sequence which includes the ACS sequence; white triangle, the position of *URA3* insertion (see Pryde and Louis, 1999 for details). (B) Measurement of repression of *URA3* inserted at ACS of coreX. 10-fold dilutions were spotted on rich medium (YPD), on synthetic complete medium lacking uracil (SC-URA), and on medium containing 5-FOA. On this last medium wild-type cells bearing *URA3* inserted into ACS sequence of core X (URA3@X-ACS) are able to repress this gene as illustrated by their ability to grow on FOA-containing medium. On the contrary, minimal repression is seen in Nup84 complex mutants (Δnup145C, Δnup84, Δnup120, Δnup133). No effect on telomeric repression is seen in other mutants (Δnup170, Δnup53). Silencing defects are complemented by full-length (FL) or the carboxy-terminal encoding part (C) of corresponding wild-type gene; Δnup133 silencing defect are complemented both by the wild-type gene (FL) or the nup133ΔN separation-of-function mutant (ΔN) that clusters NPCs (see Doye et al., 1994 for details). (C) Quantification of silencing defects. Cells were grown in nonselective conditions and 10-fold dilutions were plated onto YPD and medium containing 5-FOA.

(Fig. 2 B and unpublished data). This shows that a component of the Nup84 complex is required for efficient repair by NHEJ in subtelomeres. However, when the frequency of repair events is calculated among the survivors, similar values are obtained in wild-type and Δnup145C mutant strains (respectively 29% ± 7 and 25% ± 7), indicating that when repair of the DSB allows colony formation, the ratio of NHEJ to other mechanisms is the same in both backgrounds. 21 of these subtelomeric NHEJ events that occurred in Δnup145C mutants were sequenced, and repair event corresponded in all cases to NHEJ involving only minor rearrangements (Fig. 3). The majority of the cases (60%) correspond to a ligation between the two cut sites with insertion of two nucleotides, as already observed in a wild-type context (type II in Fig. 3 and in Ricchetti et al., 2003). The remaining cases (40%) correspond to a major resection of both I-SceI cutting sites, which was not previously described (therefore named type VII in Fig. 3).

We then analyzed the nature of non-NHEJ events at the L1 locus. The absolute frequency of these events (i.e., the number of events calculated on the total number of plated cells) is 4% in the wild-type strain, and drops to 0.25% in the Δnup145C strain (Fig. 2 B). Comparison of the Southern blot patterns (as in Ricchetti et al., 2003) of repaired chromosomes in wild-type and Δnup145C cells shows only minor variations in the frequencies of different types of repair, and no novel pattern in the mutant (unpublished data).

The repair machinery is not affected in a Δnup145C mutant strain

The observation that DSB repair is efficient in NPC mutants when the DSB is generated in a central region of a chromosome argues against a defect in nuclear transport of enzymes involved in the repair pathways. Nonetheless, we designed several experiments to confirm this. First, we studied cell survival and DSB repair using a similar experimental setup, but in which expression of I-SceI endonuclease is driven from the gene, flanked by two I-SceI cutting sites, integrated on chromosome XV at the central *ADE2* locus (Karathanasis and Wilson, 2002). In this system, the presence of an *ade2-K1* mutated allele inserted into *CAN1* (*YEL063c*) 31.7kb from telomere V-L allows visualization of GC events. In these strains, induction of I-SceI expression leads to loss of the *URA3* marker in 95% of cells. As was observed for a DSB generated in a central domain of chromosome XI, cell survival is similar in both wild-type and Δnup145C strains (Fig. 2 A and Table I). Frequencies of repair either by NHEJ or GC are also unchanged, indicating that, in the Δnup145C strain, the repair machinery is functional and has access to a central chromatin domain (Fig. 2 C and Table I). We next asked how a subtelomeric DSB can be repaired when homologous sequences are present. We thus constructed a diploid strain homozygous for the Δnup145C deletion and heterozygous for the cassette inserted at the subtelomeric L1 position. Cell survival after induction of the DSB was high in both wild-type and homozygous Δnup145C (91.5% ± 6.9

Figure 5. **Δesc1 is defective for telomere tethering and subtelomeric DSB repair.** (A) The proportion of tagged telomere XI-L in nuclear space was quantified as in Fig. 1 B. Light gray, peripheral volume; dark gray, internal volume. Bars represent the 95% confidence interval. (B) Survival to subtelomeric DSB is represented as colony forming units (CFU) as in Fig. 2 A and expressed in percentages (%). Values obtained for wild-type (WT, white) and Δesc1 (checkered) are shown. (C) Measurement of repression of *URA3* inserted at ACS of coreX of telomere XI-L as in Fig. 4. 10-fold dilutions were spotted on rich medium (YPD), on synthetic complete medium lacking uracil (SC-URA), and on medium containing 5-FOA.
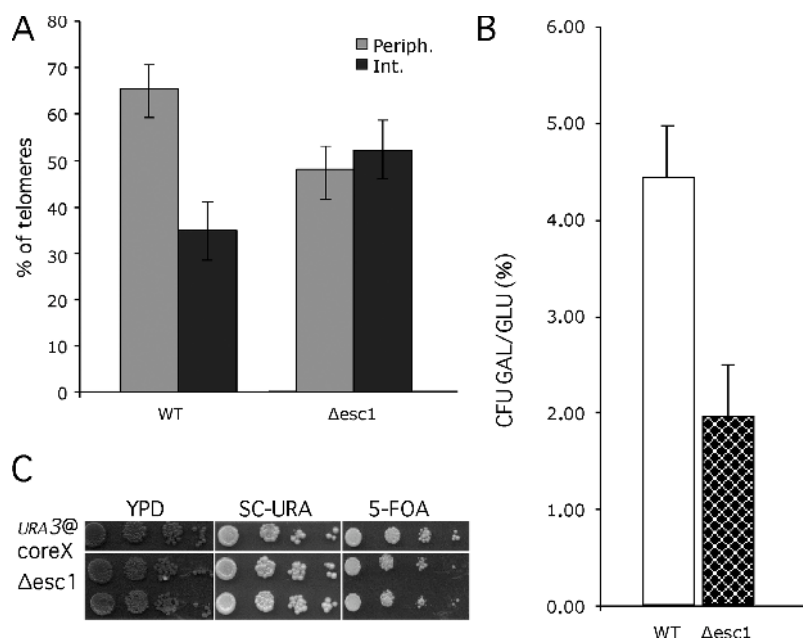
and 84% ± 11.4) with a cutting efficiency of 100%. This indicates that the inability to repair a subtelomeric DSB observed in a haploid Δnup145C strain is overtaken in a diploid strain. Finally, we used an assay that relies on the in vivo repair of a linearized plasmid required for its propagation in yeast cells (Fig. 2 C; Teo and Jackson, 1997). Because the DSB is generated in a region that is not homologous to the yeast genome, repair operates only through NHEJ. We determined the number of transformants recovered after transformation with a linearized and purified ARS-CEN-URA3 plasmid (pRS316; Sikorski and Hieter, 1989) relative to an uncut control both in wild-type and Δnup145C strains (Fig. 2 C). Restrictions leaving either 5′ overhangs (HindIII) or blunt ends (SmaI) were chosen. No differences in efficiency recovery were observed in both strains for these two types of ends, although SmaI linearized plasmid was less efficiently repaired (WT 2.1% ± 0.7; Δnup145C 2.9% ± 0.2) than HindIII (WT 24.2% ± 7.8; Δnup145C 16.5 ± 7.8), as expected (Hegde and Klein, 2000). All the above results indicate that the repair machinery is functional in Δnup145C, and therefore deficiencies in subtelomeric repair cannot be explained by a general deficiency of repair in the mutant.

Nup84p complex affects subtelomeric silencing

Because repair of a subtelomeric DSB is affected when members of the Nup84 complex are mutated, we analyzed whether silencing of subtelomeric chromatin is affected in these mutants. XI-L subtelomere was shown to be one of the most efficiently silenced subtelomeres (Pryde and Louis, 1999). Transcriptional silencing of a *URA3* marker integrated into this subtelomeric region is measured by counting the fraction of cells that are able to grow in the presence of 5-fluoro-orotic acid (5-FOA), a toxic analogue of uracil. Reverse growth of 5-FOA–resistant clones on medium lacking uracil verifies that resistance is due to subtelomeric silencing rather than mutation of the *URA3* gene.

Compared with the wild-type strain, disruption of Nup84 complex (i.e., Δnup145C, Δnup84, Δnup120, and Δnup133) reduces *URA3* silencing with variable strength, leading to very little or partial cell growth on 5-FOA (Fig. 4). On the contrary, silencing of native subtelomere XI-L remains intact when other nucleoporin genes (i.e., Δnup170 and Δnup53) are disrupted. Furthermore, silencing was restored when the corresponding wild-type nucleoporin was used for complementation, as shown for *NUP145C*, *NUP84*, and *NUP133* (Fig. 4). These results show that defects in telomere position effect (TPE) are specific for the Nup84 complex. In addition, transcomplementation of silencing defects by the *nup133ΔN* mutant, lacking the amino-terminal encoding part of Nup133p, which only affects NPC clustering (Doye et al., 1994), indicates that NPC distribution is not involved in the silencing defects observed for native telomere XI-L. We then asked whether defect in silencing corroborated with a delocalization of Sir3p. This was monitored by microscopy using a Sir3-GFP fusion protein; addition of the GFP moiety to the COOH terminus of Sir3p having no effect on TPE of native subtelomere XI-L (Fig. S2 A). In a wild-type strain Sir3-GFP localizes in few dots (4–6) located at the nuclear periphery (Fig. S2 B). In Δnup145C or Δnup84 mutants, a nucleoplasmic staining is visible and Sir3-GFP localizes to an increased number of foci (6–8), indicating a partial delocalization of Sir3-GFP in Nup84 complex mutants that may be responsible for the defect in TPE.

Esc1p affects subtelomeric repair and telomere positioning

We have established above (see previous paragraphs) Introduction or see previous paragraph that the Nup84 complex is required for telomere XI-L localization, subtelomeric DSB repair, and silencing. To define whether requirement of peripheral localization for efficient repair of subtelomeric DSBs is a general phenomenon or a specificity of the Nup84 complex, we decided

to analyze a mutant external to NPCs, with no known role in repair, that would disrupt telomere positioning. We have chosen Esc1p, a nuclear periphery protein that interacts with Sir4p and tethers native telomere XIV-L and truncated telomere VI-R (see Introduction and Andrulis et al., 2002; Taddei et al., 2004). As shown in Fig. 5 A, only 47.90% (±6.3, $n = 311$) of tagged telomere XI-L are found in the outmost external volume of $\Delta esc1$ nuclei, indicating that Esc1p is also required for tethering this telomere end. Strikingly, cell survival to a subtelomeric DSB is decreased by ∼50% in an $\Delta esc1$ mutant (Fig. 5 B). Thus, the lack of telomeric positioning at the nuclear periphery is again correlated with inefficient subtelomeric DSB repair. Furthermore, we have found that deletion of *ESC1* induces only a minor reduction on silencing efficiency of subtelomere XI-L, as previously published for other telomeres (Fig. 5 C; Andrulis et al., 2002; Taddei et al., 2004). This result allows the separation of the function of chromatin silencing with the one of chromatin repair and suggests that only chromatin positioning at the periphery is important for subtelomeric DSB repair.

Discussion

In this work we show that a central subcomplex of the NPC has a key role in the functional organization of the nuclear periphery. This is manifested by its capacity to anchor telomere XI-L at the nuclear periphery, to maintain a repressive environment for subtelomere silencing, and to participate in subtelomeric chromatin repair. These results suggest that telomere anchoring, and maybe clustering, are important for the repair of DNA breaks occurring in these regions and thus for chromosome integrity.

Our data corroborate and extend previous observations obtained for localization of native telomeres (Hediger et al., 2002a,b; Taddei et al., 2004; Bystricky et al., 2005). Most of these in vivo studies rely on quantitative analyses of the position of a fluorescent locus in the focal plane. Our analyses take into account the position of the locus in the volume of the nuclear space, and thus give an unprecedented level of positional knowledge (see also Chubb et al., 2002; Bressan et al., 2004; Cremer et al., 2004; Bystricky et al., 2005). We were able to show that tel XI-L behaves like native telomere XIV-L and VI-R, because it localizes at the periphery in a yKu70p- and Sir4p-dependent fashion, although the relative dependencies during the cell cycle for each of these proteins has not been addressed here. In addition, we show that anchoring of telomere XI-L requires the Nup84 subcomplex. Whether Nup84-dependent localization is restricted to chromosome XI-L or whether this is a shared pathway for other telomeres remains to be established, variable behaviors among native ends being probable. It is intriguing that, although required for peripheral tethering of telomeres, neither yKu70p nor Sir4p are proteins of the nuclear envelope. Sir4p was shown, however, to interact with Esc1p, a protein required for plasmid partitioning, that may interact with the nuclear envelope (Andrulis et al., 2002; Taddei et al., 2004). Nuclear pores, through the Nup84 subcomplex, now appear as serious candidates for nuclear envelope targets for telomeres that could either link yKu70p, as combined mutations of yKu and Nup84 suggest, Esc1p, or an as yet undiscovered protein(s).

The role of nuclear pores in telomere anchoring has been debated. On one hand, $\Delta nup145C$ has been described as a mutant that induces delocalization of telomeres and disintegration of telomeric clusters as measured by FISH with subtelomeric Y′ probes (Galy et al., 2000), a genetic element present on two thirds of subtelomeres in the *S. cerevisiae* sequenced strain S288C and absent in telomere XI-L studied here (Louis and Haber, 1990); on the other hand, colocalization between clustered nuclear pores (in a $\Delta nup133$ background) and the telomere-binding proteins Rap1p or Sir4p foci has rarely been observed, arguing against anchoring by the pore (Hediger et al., 2002a). However, the localization of individual native telomeres in nuclear pore mutants has not been addressed in any of these studies. We show that mutants of the Nup84 complex are defective in telomere tethering. Localization of a functional GFP-tagged version of the Sir3p silencing factor suggests, however, that this protein is partially delocalized in Nup84 complex mutants, with an increased number of visible Sir3p foci; because Sir3p binds to telomeres, it is indicative of a splitting up—but not disappearance—of telomere clusters. Whether individual, untethered telomeres remain clustered with Sir3p, Rap1p, Sir4p, or Y′ subtelomeric foci is an open question that requires first of all the determination of the telomeres constituent of each focus. All these results suggest, however, that clustering and tethering may be uncoupled, a notion that is reinforced by the observation that the clusters of telomeres can be displaced from nuclear envelope in $\Delta ku70$ mutants (Laroche et al., 1998).

Telomeric anchoring is not the only function of the inner nuclear envelope. It is well established that periphery is important for the establishment of a transcriptionally repressive environment. Transcriptional repression appears to be due to a specialized chromatin structure found in *S. cerevisiae* in the regions close to the nuclear periphery; i.e., the chromatin close to telomeres and to the silent mating type cassettes *HML* and *HMR*. Current models suggest that TPE involves binding of Rap1p to TG1-3 telomeric repeats that in turn helps to recruit Sir proteins required for subsequent proximal histone deacetylation (for reviews see Grunstein, 1997; Shore, 2000; Gasser and Cockell, 2001; Rusche et al., 2003). It is proposed that local enrichment of Sir proteins at the nuclear periphery is helped by telomere clustering. We establish here that at least for the native subtelomere XI-L, the Nup84 complex has a role in repression that does not depend on NPC clustering. This is in agreement with our previous finding that Seh1p, which also belongs to the Nup84 complex, affects subtelomeric silencing (Teixeira et al., 2002). Effects on silencing were, however, variable among Nup84 complex mutants, reflecting the relative functional importance of each entity, maybe linked to differential positioning of these proteins inside the complex (Lutzmann et al., 2002).

Paradoxically, NPCs have recently been shown to also play a role in protecting chromatin from transcriptional repression (Ishii et al., 2002; Casolari et al., 2004; Menon et al., 2005). Boundary proteins that prevent the spreading at *HML* include the NPC protein Nup2p (Ishii et al., 2002). Using genomic localization analysis, Mlp1p, Mlp2p, Nup2p, and Nup60p, but not Nup84p and Nup145Cp, were preferentially found associated with highly transcribed genes that tend to have Rap1p binding

sites (Casolari et al., 2004). On the other hand, *RAP1*-dependent transcriptional activation involves members of the Nup84 complex (Menon et al., 2005). This indicates that NPCs, through the binding of the multifunctional regulator Rap1p, have a dual role toward the transcriptional state of the chromatin and may influence organization of the nuclear periphery by partitioning active and inactive regions. Another possibility could be that NPCs are not all equivalent toward the transcriptional status of a chromosome. In any case, interaction of genes with NPCs offers a new, and not fully understood, level of gene regulation.

Previous work by Ricchetti et al. (2003) showed that DSB repair efficiency depends on the position of the DSB along the chromosome, an increased rate of survival being observed when DSBs were subtelomeric, due to NHEJ and the existence of additional mechanisms of repair including HR between repeated sequences shared by different subtelomeres. The increase in cell survival after a subtelomeric DSB was still low, possibly as a result of both limited length and level of sequence identity between these repeated sequences, or as a result of chromatin composition in that region (Ricchetti et al., 2003). Telomere tethering and/or clustering was also proposed to act as barriers to recombination between telomeric and internal chromatin in other work (Pryde and Louis, 1999). In fact, we have shown that release from the periphery does not improve cell survival to a subtelomeric DSB, but on the contrary diminishes the capacity to form colonies after DNA damage. We excluded that this decreased rate of survival is due to a defective checkpoint that would impede cellular recovery to the DSB. The observed decrease in cell survival might be due to a deficient DSB repair specific to subtelomeric regions. We do not know, however, at which precise level repair is affected; it could either be a defect in repair kinetics or in other processes like the choice of the partner (Aylon and Kupiec, 2003). Subtelomere tethering at the nuclear periphery appears as a requirement for their capacity to repair genomic injuries occurring therein, an observation reminiscent of the proposed role of telomeres clustering in facilitating recombination between subtelomeres of other organisms (Freitas-Junior et al., 2000; Figueiredo et al., 2002; Tuzon et al., 2004).

It is noteworthy that three mutants of the Nup84 complex, namely Δ*nup84*, Δ*nup133*, and Δ*nup120* were found to be synthetically lethal with genes involves in replication (Δ*rad27*) and repair (Rad52 pathway) (Loeillet et al., 2005). This genetic interaction was correlated with an increased number of Rad52-YFP foci. Because spontaneous DSBs arising during mitotic DNA synthesis may be repaired though recombination, it was proposed that Nup133p may be important for this process. Our data extend this observation, showing that the Nup84 complex, through Nup84p, Nup120p, Nup133p, and Nup145Cp, is indeed important for repair, but restricted to the subtelomeric domain. Whether Rad52-YFP foci correspond to recruitment of the repair machinery at the periphery remains an open question. Nup84p, Nup133p, and Nup120p nucleoporins were also found in genome-wide screens searching for DNA damage pathways (resistance to γ radiations, sensitivity to MMS or bleomycin; (Bennett et al., 2001; Chang et al., 2002). It was shown in particular that recombination between donors and the mating type

cassette, allowing for repair of a DSB initiated by HO, was impossible in a Δnup84 mutant (Bennett et al., 2001). This was interpreted as the putative consequence of a defect in nuclear transport of repair enzymes. In light of our results, we favor a hypothesis in which repair of *HML* or *HMR*, which are subtelomeric, could not operate because the nuclear periphery is perturbed in the Δnup84 mutant. It should be noted that most of the constituents of Nup84p complex, when deleted, lead to a defect in NPC positioning in the plane of the nuclear envelope (Doye et al., 1994; Heath et al., 1995; Siniossoglou et al., 1996; Teixeira et al., 1997). It is possible that NPC clustering is in part responsible for the defects observed here. However, studies with Δnup145C were performed at 25°C, a permissive temperature at which not only nuclear transport is normal, but also NPC clustering is not complete (unpublished data) and NPC clustering was excluded as a cause of increased Rad52 foci (Loeillet et al., 2005). Altogether, this suggests that telomere anchoring through the Nup84 complex is necessary for the efficient repair of DSBs occurring in these regions.

The finding that deletion of *ESC1*, which encodes a nonchromatin protein associated with the nuclear periphery (Andrulis et al., 2002; Taddei et al., 2004), affects both telomere tethering and efficiency of subtelomeric DSB repair, substantiates our findings on the functional importance of chromatin organization at the nuclear periphery. Furthermore, as previously shown, chromatin anchoring is found to occur independently of transcriptional repression in Δesc1 mutant (Andrulis et al., 2002; Taddei et al., 2004); this allows the uncoupling of silencing and the chromatin modifications inherent to it, and the defects observed here in subtelomeric repair.

Despite the importance of spatial chromatin organization, little is known about the molecular principles that define its organization.

A key role for nuclear envelope proteins is however substantiated, in particular in organisms in which mitosis is open; nuclear lamina proteins and the NPC proteins, through the mammalian orthologue of the Nup84 complex, vNup107, were shown to initiate the first steps of post-mitotic chromatin reassembly (Harel et al., 2003; Walther et al., 2003). Another role for NPCs in defining nuclear environments favorable for DSB repair is highlighted here, maybe through nonrandom chromatin organization as is suggested for telomere clustering, origin firing, and pairing between silenced and nonsilenced mating type cassettes.

Materials and methods

Yeast strain construction
All the strains studied here are derived from the sequenced strain S288C, and genotypes are summarized in Table II. Nucleoporin, *yKU70*, *SIR4*, and *ESC1* disruptions were introduced either by transformation with kanMX *HIS3* or a *TRP1* PCR fragment allowing for single step disruption (Baudin et al., 1993), or by mating and sporulation. Deletion of *NUP145C* was defined according to Teixeira et al. (1997). All gene deletions were verified by Southern blot by using wild-type genes as probes. Tagging of telomere XI-L for in vivo localization was performed by integrating 112*tetO* repeats at 3.5 kb from telomere. The yeast integrative plasmid pRS306 (Sikorski and Hieter, 1989) containing 112 42-bp fragments including the 19-bp palyndromic *tetO*2 sequence (hereafter referred to as *tetO* repeats) was initially obtained from K. Nasmyth (Research Institute of

Table II. **Strains used in this work**

Strain name	Genotype	Reference
FYBL1-8B/Ai0611	MATa, ura3-Δ851, leu2Δ1, his3Δ200, lys2Δ202, ykl222c::csURA3cs[a]	(Ricchetti et al., 2003)
YEF402	FYBL1-8B/Ai0611/Δnup145C::kanMX4	This work
YPT005	MATa, ura3, trp1-Δ63, leu2, his3, ykl222c::csURA3cs, Δnup84::kanMX4[b]	This work
YPT009	MATa, ura3, trp1-Δ63, leu2, his3, ykl222c::csURA3cs, Δnup170::kanMX4[b]	This work
YPT084	MATa, ura3, trp1-Δ63, leu2, his3, ykl222c::csURA3cs, Δnup133::kanMX4[b]	This work
YPT090	FYBL1-8B/Ai0611/Δnup120::kanMX4	This work
FYBL1-8B/Bn001	MATa, ura3-Δ0, leu2Δ1, his3Δ200, lys2Δ202, ykl201c::csURA3cs	(Ricchetti et al., 2003)
YEF460	FYBL1-8B/Bn001/Δnup145C::kanMX4	This work
YPT007	MATa, ura3, trp1-Δ63, leu2, his3 ykl201c::csURA3cs, Δnup84::kanMX4[b]	This work
YPT012	MATa, ura3, trp1-Δ63, leu2, his3, Δnup170::kanMX4[b]	This work
YW656	Matα, ura3Δ0, leu2Δ0, his3Δ1, met15Δ0, can1Δ::ade2-K1, ade2::SD2-::GAL-Iscel::URA3	(Karathanasis and Wilson, 2002)
YEF458	YW656/Δnup145C::kanMX4	This work
YW 969	Matα, ura3Δ0, leu2Δ0, his3Δ1, met15Δ0, can1Δ::ade2-K1, ade2::SD2-::GAL-Iscel::URA3	(Karathanasis and Wilson, 2002)
YEF456	YW969/Δnup145C::kanMX4	This work
YEF472a	MATa, ura3Δ851, leu2Δ1, his3Δ200, lys2Δ202, ykl222c::csURA3cs::tet0112::NATMX, LEU2::tetR-GFP	This work
YEF473a	YEF472a/Δnup145C::kanMX4	This work
YEF499-8A	YEF472a/Δku70::kanMX4	This work
YPT030	MATa, ura3, leu2, his3, lys2, ykl222c::csURA3cs::tet0112::NATMX, LEU2::tetR-GFP, Δnup84::kanMX4[b]	This work
YPT082	YEF472a/Δnup133::kanMX4	This work
YPT087	YEF472a/Δnup120::kanMX4	This work
YPT065	MATa ura3, trp1Δ63, leu2, his3, lys2, ade2Δ, ykl222c::csURA3cs::tet0112::NATMX, LEU2::tetR-GFP, Δesc1::TRP1[b]	This work
YPT071	YEF472a/Δsir4::kanMX4	This work
YEF548	MATa, ura3-Δ851, leu2Δ-1, his3Δ200, lys2Δ-202, ykl222c::csURA3cs::tet0112::NATMX, LEU2::tetR-GFP, Δnup145C::KANMX4, Δku70::hph	This work
FEP100	MATa, ura3-52, leu2Δ1, ade2Δ, can1-1, tel XI coreX::URA3	(Pryde and Louis, 1999)
YEF486-6C	FEP100/Δnup145C::kanMX4	This work
YPT001	MATα, ura3, leu2, ade2Δ, telXI coreX::URA3, Δnup84::kanMX4[b]	This work
YPT003	MATα, ura3, leu2, ade2Δ, telXI coreX::URA3, Δnup170::kanMX4[b]	This work
YPT0034	MATα, ura3, leu2, ade2Δ, telXI coreX::URA3, Δnup53::kanMX4[b]	This work
YPT036	MATα, ura3, leu2, ade2Δ, telXI coreX::URA3, Δnup120::kanMX4[b]	This work
YPT038	MATα, ura3, leu2, ade2Δ, telXI coreX::URA3, Δnup133::kanMX4[b]	This work
YEF505	MATα, ura3, leu2, ade2Δ, telXI coreX::URA3, SIR3-GFP::TRP1	This work
YEF506	MATα, ura3-52, trp1Δ63, ade2Δ, his3Δ200, SIR3-GFP::TRP1, Δhdf1::hphMX4	This work
YEF508	MATa, ura3-52, trp1Δ63, leu2Δ1, ade2Δ, SIR3-GFP::TRP1, Δnup84::kanMX4	This work
YEF509	MATa, ura3-52, trp1Δ63, leu2Δ1, ade2Δ, his3Δ200, SIR3GFP::TRP1, Δnup145C::kanMX4, telXI coreX::URA3	This work

[a]cs indicates cutting sites for the I-SceI endonuclease.
[b]These strains are issued from matings with strains derived from BY4742 background (Brachmann et al., 1998); alleles for his3, ura3, leu2, lys2 are therefore not determined.

Molecular Pathology, Vienna, Austria) (Michaelis et al., 1997). Gene natMX4 coding for nourseotricin resistance was linked to the *tetO* repeats, by cloning a BglII-AatII natMX4 containing fragment from pAG25 (Goldstein and McCusker, 1999) into pRS306-*tetO*112. The resulting plasmid was linearized by StuI and used to transform strain FYBL1-8B/Ai0611 (Ricchetti et al., 2003), allowing for insertion of *tetO* repeats at *URA3*. *tetO* insertion and size of the repeats were checked by Southern blot. Digestion by EcoRV of modified YIplac128 plasmid (Michaelis et al., 1997) allowed integration of SV40NLS-TetR::GFP at *leu2Δ1* locus. The strain was verified by Southern blot using *LEU2* as a probe and disrupted either for *NUP145C*, *NUP120*, *NUP133*, or *SIR4* by transformation or for *NUP84*, *ESC1*, or *yKU70* by mating.

Fluorescence observation and QuIA analysis

Haploid cells tagged by *tetO* repeats on chromosome XI-L (see Table II) were grown to exponential phase at 25°C in 5ml of YPD. When concentration reached $1–2 \times 10^6$ cells/ml, cells from 1 ml aliquots were washed in synthetic complete medium and resuspended into 500 μl of the same medium. 5 μl were spotted onto slides, covered by a thin layer of agar (1.5% agar in synthetic complete medium). Images were captured with an UltraView RS Nipkow-disk confocal system (Perkin-Elmer) and controlled by PE-viewer software. A 100× objective (Plan Apo, 1.4 NA, oil immersion; Carl Zeiss MicroImaging, Inc.) was used. The pixel size is 65.8 nm. Stacks with a slice spacing of 200 nm were taken using a laser excitation of 488 nm with an acquisition time of 200 ms each. An analysis of each projected stack was performed with QuIA software. This software relies on the quantitative detection of the labeled chromosomal locus via its 3D coordinates (X, Y, Z) in the nuclear space by a multi-resolution method using a 3D wavelet transformation, allowing to correlate information from different subbands of analysis and to select spot-like structures only within the nuclear volume (Olivo-Marin, 2002). The output of the detection step are the coordinates of the center of the chromosomal locus and of the nucleus, from which a first estimate of their relative distance is computed, before correction of Z distortion. TetR-GFP background allows for nucleoplasm detection and calculation of R_{est}, i.e., the mean of all radii on the median focal plane, assuming the nucleus is spherical. In wild-type cells, border of TetR-GFP background coincides with Nup49-GFP staining. Z-distortion and Z-detection artifacts are corrected thanks to the values obtained from localization of a GFP fusion with Spc29p, a single pole body (SPB) protein. In yeast, the SPB is embedded in the nuclear envelope. Without any Z distortion, the

distance between the SPB and the center of nucleus, normalized by the R_{est} value (d_{SPB}/R_{est}), should be constant whatever the Z coordinate of the SPB. On the contrary, the observed distribution d_{SPB}/R_{est} increases with the distance along the Z-axis of the SPB from the median plane of the nucleus. This distribution is best fitted by the second-degree polynomial curve: $d_{SPB}/R_{est} = 0.3309(Z_{SPB} - Z_{nucleus\ center})^2 + 0.0129(Z_{SPB} - Z_{nucleus\ center}) + 0.8457$. This equation was used to determine the compensatory term to be removed from all the measured radial distances between the barycentre of $tetO$ locus and of the nucleus (d_{tetO}) and normalized by the R_{est} value (dtetO/Rest). Thus the corrected ratio, termed relative 3D position (R3Dp) is $d_{tetO}/R_{est} = d_{tetO}/R_{est} - (0.3309(Z_{TetO} - Z_{nucleus\ center})^2 + 0.0129(Z_{tetO} - Z_{nucleus\ center}))$. In each strain, percentages of cells according to their R3Dp are then either distributed in two zones of equal volume (i.e., 50% of the volume each, the outmost external one defined as the peripheral one) or presented as a cumulative distribution function (CDF), allowing for a Kolmogorov-Smirnov test that determines the statistical differences between two distributions. Note that the depth of the most external volume of a sphere divided in two equal volumes is similar to the depth of the most external area of a circular surface divided in three equal areas (see Hediger et al., 2002b). Analyses were performed on at least 200 nuclei in at least three independent experiments. The average nuclear radius in mutant cells versus WT cells was measured and shown to be similar between strains (0.97 μm ± 0.02, in WT and Δesc1; 0.98 μm ± 0.03 in Δsir4 and Δnup133; 0.99 ± 0.11 in Δnup145C; 1.02 ± 0.04 in Δku70; 1.07 ± 0.04 in Δku70 Δnup145; 0.92 ± 0.02 in Δnup120 and 1.15 ± 0.13 in Δnup84). In Δnup84 mutant, cell morphology is more variable, but distorted cells do not exceed 10% of the entire population.

Silencing assays

Silencing of a *URA3* marker inserted at the core X of chromosome XI-L (Pryde and Louis, 1999) was scored after growth of strains in nonselective conditions (YPD) to mid-log phase. 10-fold serial dilutions were made and spotted or plated to either SC-URA or plates containing 5-FOA. The percentage of cells giving rise to 5-FOA resistant colonies was calculated after 2–3 d of growth.

Induction of I-SceI DSBs in vivo

Wild-type, Δnup145C, Δnup84, Δnup133, Δnup120, Δnup170, or Δesc1 strains containing the *URA3* cassette flanked by two inverted I-SceI cutting sites at different positions along chromosome XI were transformed by the I-SceI expression plasmids, either pPEX7 (Fairhead and Dujon, 1993) or pPEX14 (this paper). Both plasmids carry the I-SceI ORF controlled by a galactose-inducible promoter and a *leu2d* marker. pPEX14 corresponds to a version of pPEX7 in which a *TRP1* marker is inserted, allowing for efficient selection of transformants on SC-TRP. Induction of DSB was performed as in Ricchetti et al. (2003). Experiments were repeated at least five times with at least two independent pPEX transformants each time.

PCRs and genomic analyses

Analyses of repair events at the molecular level were done according to Ricchetti et al. (2003). The frequency of repair events was calculated as the ratio of the number of these events divided by the number of colonies growing on galactose. The absolute frequencies were determined in each strain by dividing the previous value by the number of plated cells on glucose medium.

Online supplemental material

Fig. S1: Nup84 complex is required for tethering of tel-XIL at the periphery: CDF values. Fig. S2: Δnup145C mutant is not defective in cell cycle arrest due to subtelomeric DSB. Fig. S3: Nup84 complex partially affects Sir3p localization. Online supplemental material available at http://www.jcb.org/cgi/content/full/jcb.200505159/DC1.

References

Andrulis, E.D., A.M. Neiman, D.C. Zappulla, and R. Sternglanz. 1998. Perinuclear localization of chromatin facilitates transcriptional silencing. *Nature.* 394:592–595.

Andrulis, E.D., D.C. Zappulla, A. Ansari, S. Perrod, C.V. Laiosa, M.R. Gartenberg, and R. Sternglanz. 2002. Esc1, a nuclear periphery protein required for Sir4-based plasmid anchoring and partitioning. *Mol. Cell. Biol.* 22:8292–8301.

Aten, J.A., J. Stap, P.M. Krawczyk, C.H. van Oven, R.A. Hoebe, J. Essers, and R. Kanaar. 2004. Dynamics of DNA double-strand breaks revealed by clustering of damaged chromosome domains. *Science.* 303:92–95.

Aylon, Y., and M. Kupiec. 2003. The checkpoint protein Rad24 of *Saccharomyces cerevisiae* is involved in processing double-strand ends and in recombination partner choice. *Mol. Cell. Biol.* 23:6585–6596.

Baudin, A., O. Ozier-Kalogeropoulos, A. Denouel, F. Lacroute, and C. Cullin. 1993. A simple and efficient method for direct gene deletion in *Saccharomyces cerevisiae. Nucleic Acids Res.* 21:3329–3330.

Bennett, C.B., L.K. Lewis, G. Karthikeyan, K.S. Lobachev, Y.H. Jin, J.F. Sterling, J.R. Snipe, and M.A. Resnick. 2001. Genes required for ionizing radiation resistance in yeast. *Nat. Genet.* 29:426–434.

Bosco, G., and J.E. Haber. 1998. Chromosome break-induced DNA replication leads to nonreciprocal translocations and telomere capture. *Genetics.* 150:1037–1047.

Brachmann, C.B., A. Davies, G.J. Cost, E. Caputo, J. Li, P. Hieter, and J.D. Boeke. 1998. Designer deletion strains derived from *Saccharomyces cerevisiae* S288C: a useful set of strains and plasmids for PCR-mediated gene disruption and other applications. *Yeast.* 14:115–132.

Bressan, D.A., J. Vazquez, and J.E. Haber. 2004. Mating type-dependent constraints on the mobility of the left arm of yeast chromosome III. *J. Cell Biol.* 164:361–371.

Bystricky, K., T. Laroche, G. van Houwe, M. Blaszczyk, and S.M. Gasser. 2005. Chromosome looping in yeast: telomere pairing and coordinated movement reflect anchoring efficiency and territorial organization. *J. Cell Biol.* 168:375–387.

Casolari, J.M., C.R. Brown, S. Komili, J. West, H. Hieronymus, and P.A. Silver. 2004. Genome-wide localization of the nuclear transport machinery couples transcriptional status and nuclear organization. *Cell.* 117:427–439.

Chang, M., M. Bellaoui, C. Boone, and G.W. Brown. 2002. A genome-wide screen for methyl methanesulfonate-sensitive mutants reveals genes required for S phase progression in the presence of DNA damage. *Proc. Natl. Acad. Sci. USA.* 99:16934–16939.

Chubb, J.R., S. Boyle, P. Perry, and W.A. Bickmore. 2002. Chromatin motion is constrained by association with nuclear compartments in human cells. *Curr. Biol.* 12:439–445.

Cremer, T., and C. Cremer. 2001. Chromosome territories, nuclear architecture and gene regulation in mammalian cells. *Nat. Rev. Genet.* 2:292–301.

Cremer, T., K. Kupper, S. Dietzel, and S. Fakan. 2004. Higher order chromatin architecture in the cell nucleus: on the way from structure to function. *Biol. Cell.* 96:555–567.

Doye, V., R. Wepf, and E.C. Hurt. 1994. A novel nuclear pore protein Nup133p with distinct roles in poly(A)+ RNA transport and nuclear pore distribution. *EMBO J.* 13:6062–6075.

Fairhead, C., and B. Dujon. 1993. Consequences of unique double-stranded breaks in yeast chromosomes: death or homozygosis. *Mol. Gen. Genet.* 240:170–178.

Fairhead, C., B. Llorente, F. Denis, M. Soler, and B. Dujon. 1996. New vectors for combinatorial deletions in yeast and for gap-repair cloning using 'split-marker' recombination. *Yeast.* 12:1439–1457.

Feuerbach, F., V. Galy, E. Trelles-Sticken, M. Fromont-Racine, A. Jacquier, E. Gilson, J.C. Olivo-Marin, H. Scherthan, and U. Nehrbass. 2002. Nuclear architecture and spatial positioning help establish transcriptional states of telomeres in yeast. *Nat. Cell Biol.* 4:214–221.

Figueiredo, L.M., L.H. Freitas-Junior, E. Bottius, J.C. Olivo-Marin, and A. Scherf. 2002. A central role for *Plasmodium falciparum* subtelomeric regions in spatial positioning and telomere length regulation. *EMBO J.* 21:815–824.

Freitas-Junior, L.H., E. Bottius, L.A. Pirrit, K.W. Deitsch, C. Scheidig, F. Guinet, U. Nehrbass, T.E. Wellems, and A. Scherf. 2000. Frequent ectopic recombination of virulence factor genes in telomeric chromosome clusters of *P. falciparum*. *Nature*. 407:1018–1022.

Galy, V., J.C. Olivo-Marin, H. Scherthan, V. Doye, N. Rascalou, and U. Nehrbass. 2000. Nuclear pore complexes in the organization of silent telomeric chromatin. *Nature*. 403:108–112.

Gasser, S.M., and M.M. Cockell. 2001. The molecular biology of the SIR proteins. *Gene*. 279:1–16.

Goldstein, A.L., and J.H. McCusker. 1999. Three new dominant drug resistance cassettes for gene disruption in *Saccharomyces cerevisiae*. *Yeast*. 15:1541–1553.

Gotta, M., T. Laroche, A. Formenton, L. Maillet, H. Scherthan, and S.M. Gasser. 1996. The clustering of telomeres and colocalization with Rap1, Sir3, and Sir4 proteins in wild-type *Saccharomyces cerevisiae*. *J. Cell Biol.* 134:1349–1363.

Gottschling, D.E., O.M. Aparicio, B.L. Billington, and V.A. Zakian. 1990. Position effect at *S. cerevisiae* telomeres: reversible repression of Pol II transcription. *Cell*. 63:751–762.

Grunstein, M. 1997. Molecular model for telomeric heterochromatin in yeast. *Curr. Opin. Cell Biol.* 9:383–387.

Harel, A., A.V. Orjalo, T. Vincent, A. Lachish-Zalait, S. Vasu, S. Shah, E. Zimmerman, M. Elbaum, and D.J. Forbes. 2003. Removal of a single pore subcomplex results in vertebrate nuclei devoid of nuclear pores. *Mol. Cell*. 11:853–864.

Heath, C.V., C.S. Copeland, D.C. Amberg, V. Del Priore, M. Snyder, and C.N. Cole. 1995. Nuclear pore complex clustering and nuclear accumulation of poly(A)+ RNA associated with mutation of the *Saccharomyces cerevisiae* RAT2/NUP120 gene. *J. Cell Biol.* 131:1677–1697.

Hediger, F., K. Dubrana, and S.M. Gasser. 2002a. Myosin-like proteins 1 and 2 are not required for silencing or telomere anchoring, but act in the Tel1 pathway of telomere length control. *J. Struct. Biol.* 140:79–91.

Hediger, F., F.R. Neumann, G. Van Houwe, K. Dubrana, and S.M. Gasser. 2002b. Live imaging of telomeres: yKu and Sir proteins define redundant telomere-anchoring pathways in yeast. *Curr. Biol.* 12:2076–2089.

Hegde, V., and H. Klein. 2000. Requirement for the SRS2 DNA helicase gene in non-homologous end joining in yeast. *Nucleic Acids Res.* 28:2779–2783.

Ishii, K., G. Arib, C. Lin, G. Van Houwe, and U.K. Laemmli. 2002. Chromatin boundaries in budding yeast: the nuclear pore connection. *Cell*. 109:551–562.

Jin, Q.W., J. Fuchs, and J. Loidl. 2000. Centromere clustering is a major determinant of yeast interphase nuclear organization. *J. Cell Sci.* 113:1903–1912.

Karathanasis, E., and T.E. Wilson. 2002. Enhancement of *Saccharomyces cerevisiae* end-joining efficiency by cell growth stage but not by impairment of recombination. *Genetics*. 161:1015–1027.

Laroche, T., S.G. Martin, M. Gotta, H.C. Gorham, F.E. Pryde, E.J. Louis, and S.M. Gasser. 1998. Mutation of yeast Ku genes disrupts the subnuclear organization of telomeres. *Curr. Biol.* 8:653–656.

Lee, S.E., J.K. Moore, A. Holmes, K. Umezu, R.D. Kolodner, and J.E. Haber. 1998. *Saccharomyces* Ku70, mre11/rad50 and RPA proteins regulate adaptation to G2/M arrest after DNA damage. *Cell*. 94:399–409.

Lisby, M., and R. Rothstein. 2004. DNA repair: keeping it together. *Curr. Biol.* 14:R994–R996.

Lisby, M., J.H. Barlow, R.C. Burgess, and R. Rothstein. 2004. Choreography of the DNA damage response: spatiotemporal relationships among checkpoint and repair proteins. *Cell*. 118:699–713.

Loeillet, S., B. Palancade, M. Cartron, A. Thierry, G.F. Richard, B. Dujon, V. Doye, and A. Nicolas. 2005. Genetic network interactions among replication, repair and nuclear pore deficiencies in yeast. *DNA Repair (Amst.)*. 4:459–468.

Louis, E.J., and J.E. Haber. 1990. The subtelomeric Y′ repeat family in *Saccharomyces cerevisiae*: an experimental system for repeated sequence evolution. *Genetics*. 124:533–545.

Lutzmann, M., R. Kunze, A. Buerer, U. Aebi, and E. Hurt. 2002. Modular self-assembly of a Y-shaped multiprotein complex from seven nucleoporins. *EMBO J.* 21:387–397.

Maillet, L., C. Boscheron, M. Gotta, S. Marcand, E. Gilson, and S.M. Gasser. 1996. Evidence for silencing compartments within the yeast nucleus: a role for telomere proximity and Sir protein concentration in silencer-mediated repression. *Genes Dev.* 10:1796–1811.

Maillet, L., F. Gaden, V. Brevet, G. Fourel, S.G. Martin, K. Dubrana, S.M. Gasser, and E. Gilson. 2001. Ku-deficient yeast strains exhibit alternative states of silencing competence. *EMBO Rep.* 2:203–210.

Marcand, S., S.W. Buck, P. Moretti, E. Gilson, and D. Shore. 1996. Silencing of genes at nontelomeric sites in yeast is controlled by sequestration of

silencing factors at telomeres by Rap 1 protein. *Genes Dev.* 10:1297–1309.

Marshall, W.F. 2002. Order and disorder in the nucleus. *Curr. Biol.* 12:R185–R192.

Menon, B.B., N.J. Sarma, S. Pasula, S.J. Deminoff, K.A. Willis, K.E. Barbara, B. Andrews, and G.M. Santangelo. 2005. Reverse recruitment: The Nup84 nuclear pore subcomplex mediates Rap1/Gcr1/Gcr2 transcriptional activation. *Proc. Natl. Acad. Sci. USA*. 102:5749–5754.

Michaelis, C., R. Ciosk, and K. Nasmyth. 1997. Cohesins: chromosomal proteins that prevent premature separation of sister chromatids. *Cell*. 91:35–45.

Olivo-Marin, J.-C. 2002. Extraction of spots in biological images using multi-scale products. *Pattern Recognit.* 35:1989–1996.

Pryde, F.E., and E.J. Louis. 1999. Limitations of silencing at native yeast telomeres. *EMBO J.* 18:2538–2550.

Ricchetti, M., C. Fairhead, and B. Dujon. 1999. Mitochondrial DNA repairs double-strand breaks in yeast chromosomes. *Nature*. 402:96–100.

Ricchetti, M., B. Dujon, and C. Fairhead. 2003. Distance from the chromosome end determines the efficiency of double strand break repair in subtelomeres of haploid yeast. *J. Mol. Biol.* 328:847–862.

Rine, J., and I. Herskowitz. 1987. Four genes responsible for a position effect on expression from HML and HMR in *Saccharomyces cerevisiae*. *Genetics*. 116:9–22.

Rusche, L.N., A.L. Kirchmaier, and J. Rine. 2003. The establishment, inheritance, and function of silenced chromatin in *Saccharomyces cerevisiae*. *Annu. Rev. Biochem.* 72:481–516.

Sandell, L.L., and V.A. Zakian. 1993. Loss of a yeast telomere: arrest, recovery, and chromosome loss. *Cell*. 75:729–739.

Shore, D. 2000. The Sir2 protein family: A novel deacetylase for gene silencing and more. *Proc. Natl. Acad. Sci. USA*. 97:14030–14032.

Sikorski, R.S., and P. Hieter. 1989. A system of shuttle vectors and yeast host strains designed for efficient manipulation of DNA in *Saccharomyces cerevisiae*. *Genetics*. 122:19–27.

Siniossoglou, S., C. Wimmer, M. Rieger, V. Doye, H. Tekotte, C. Weise, S. Emig, A. Segref, and E.C. Hurt. 1996. A novel complex of nucleoporins, which includes Sec13p and a Sec13p homolog, is essential for normal nuclear pores. *Cell*. 84:265–275.

Smith, J.S., and J.D. Boeke. 1997. An unusual form of transcriptional silencing in yeast ribosomal DNA. *Genes Dev.* 11:241–254.

Taddei, A., F. Hediger, F.R. Neumann, C. Bauer, and S.M. Gasser. 2004. Separation of silencing from perinuclear anchoring functions in yeast Ku80, Sir4 and Esc1 proteins. *EMBO J.* 23:1301–1312.

Teixeira, M.T., S. Siniossoglou, S. Podtelejnikov, J.C. Benichou, M. Mann, B. Dujon, E. Hurt, and E. Fabre. 1997. Two functionally distinct domains generated by in vivo cleavage of Nup145p: a novel biogenesis pathway for nucleoporins. *EMBO J.* 16:5086–5097.

Teixeira, M., B. Dujon, and E. Fabre. 2002. Genome-wide nuclear morphology screen identifies novel genes involved in nuclear architecture and gene-silencing in *Saccharomyces cerevisiae*. *J. Mol. Biol.* 321:551–561.

Teo, S.H., and S.P. Jackson. 1997. Identification of *Saccharomyces cerevisiae* DNA ligase IV: involvement in DNA double-strand break repair. *EMBO J.* 16:4788–4795.

Tham, W.H., J.S. Wyithe, P. Ko Ferrigno, P.A. Silver, and V.A. Zakian. 2001. Localization of yeast telomeres to the nuclear periphery is separable from transcriptional repression and telomere stability functions. *Mol. Cell*. 8:189–199.

Tuzon, C.T., B. Borgstrom, D. Weilguny, R. Egel, J.P. Cooper, and O. Nielsen. 2004. The fission yeast heterochromatin protein Rik1 is required for telomere clustering during meiosis. *J. Cell Biol.* 165:759–765.

Walther, T.C., A. Alves, H. Pickersgill, I. Loiodice, M. Hetzer, V. Galy, B.B. Hulsmann, T. Kocher, M. Wilm, T. Allen, et al. 2003. The conserved Nup107-160 complex is critical for nuclear pore complex assembly. *Cell*. 113:195–206.